Case Studies in Thermal Engineering 8 (2016) 32–40

Contents lists available at ScienceDirect

Case Studies in Thermal Engineering

journal homepage: www.elsevier.com/locate/csite

Simulation and experimental investigation of the wavy fin-and-tube intercooler ☆

Qinguo Zhang, Sicheng Qin *, Runda Ma

School of Mechanical Science and Engineering, Jilin University, Changchun, Jilin 130022, China

ARTICLE INFO

Article history:
Received 28 August 2015
Received in revised form
6 September 2015
Accepted 9 April 2016
Available online 11 April 2016

Keywords:
Wavy fin
Porous medium
Heat transfer
Flow uniformity

ABSTRACT

In this paper, flow and heat transfer characteristics in the fin-and-tube intercooler were numerically investigated using the FLUENT software by adopting the porous medium approach, which could obtain the distributions, including temperature, pressure and non-uniform, etc. The effects of the air flow rate on the resistance characteristic and the heat transfer performance were analyzed. The simulation results show that the pressure drop and the heat transfer capacity increase with the increase of air flow rate. Simultaneously, the coolant distribution is uniform in the header with the maximum error within± 10%. Two kinds of coolant flow schemes have an important influence on heat transfer. Those results also confirm that the higher the heat transfer rate, the lower the inlet coolant temperature is. Finally, comparison results show that the numerical results based on the heat transfer model in porous medium agree well with the measured data based on the engine bench test. The conclusions of this paper are of great significance in the improvement of fin-and-tube intercooler.

1. Introduction

Intercooler as a core component of the engine has an important effect. For instance, it can lower inlet temperature and increase the density of air, in turn, increase the combustion efficiency. The experiment has proved that installing intercooler could obviously enhance engine power; meanwhile, oil-saving effect is obvious. And, still can reduce emissions, protect the environment. Therefore, studying the working performance of the intercooler is necessary.

At present, the research for the fin-and-tube radiator mainly adopts the experimental method. Dong [1] studied the thermal-hydraulic performance of a wavy fin-and-flat tube radiator. Oliet [2] and Shon [3] studied the coolant parameters in a fin-tube heat exchanger. Wen [4] and Jiao [5] and Habib [6] carried out an experimental investigation of header configuration on flow maldistribution in plate-fin heat exchanger. In recent years, with the continuous development of simulation technology, using CFD method deal with fluid flow and heat transfer is becoming more and more popular. Three-dimensional numerical study of heat transfer characteristics of radiators was carried out by researchers [7–9]. Wang [10] and Chen [11] successfully investigated the flow field and temperature field of the total helical baffle heat exchanger based on CFD analysis without using porous medium, however, it is impossible for tube-and-fin radiator. Thus, A. A. Masri [12] predicted the temperature distribution in a full scale APU SOFC short stack, which is a plate-fin radiator actually using porous medium.

☆ Fundation Item: the National Science and Technology Support Program (no. 2013BAF07B04).
* Corresponding author.
E-mail address: qsc925@hotmail.com (S. Qin).

http://dx.doi.org/10.1016/j.csite.2016.04.003

Nomenclature

b	longitudinal pitch (mm).
d	transverse pitch (mm).
Ac	minimum free flow area (m^2).
D_e	hydraulic diameter of fin entrance (mm).
M	mass flow rate (kg/s).
ΔP	pressure drop (pa).
Q	heat transfer rate (w).
t_1	inlet temperature (K).
t_2	outlet temperature (K).
F_p	fin pitch (mm).
F_h	fin height (mm).
L	fin length along the flow direction (mm).
T	temperature (k).

Dimensionless groups

Nu	Nusselt number.
Re	Reynolds number.
P_r	Prandtl number.
exp	experimental.
sim	simulation.
C	air inlet.
D	air outlet.

Greek symbols

ρ	density (kg/m^3).
λ	thermal conductivity (W/m●k).
μ	dynamic viscosity (kg/m●s).
α	corrugation angle (°).
h	heat transfer coefficient (w/m^2●k).
C_P	specific heat at constant pressure (J/kg●k).

And a good agreement between experimental data and simulation values were obtained.

At present, the fin type within the intercooler mainly uses straight fins. However, because of its excellent heat transfer performance, the applications of wavy fins are increasing. Thus, the wavy fin performance is mainly evaluated in this paper. In the present paper, the tube-and-fin intercooler was studied experimentally and numerically. The aim was to understand the flow and heat transfer characteristics in the whole cooler under different boundary conditions based on a porous media model using FLUENT software.

2. Model for whole heat exchanger simulation

2.1. Physical model

The schematic diagram of the wavy fins and tubes is shown in Fig. 1 The fin-and-tube intercooler studied in the article has a staggered tube arrangement Fluid passage regions are characterized by complex geometries due to the wavy fins, which ensure the heat transfer coefficient to be enhanced by increasing the heat transfer surface and nonuniform flow. The fins and water manifolds are assembled by braze welding process in a nitrogen atmosphere to guarantee perfect sealing. Owing to complicated 3D flow between fins and pipes, it is impossible to employ a numerical simulation method for predicting the real flow field on the overall model by software. Therefore, the real intercooler geometry is used except for

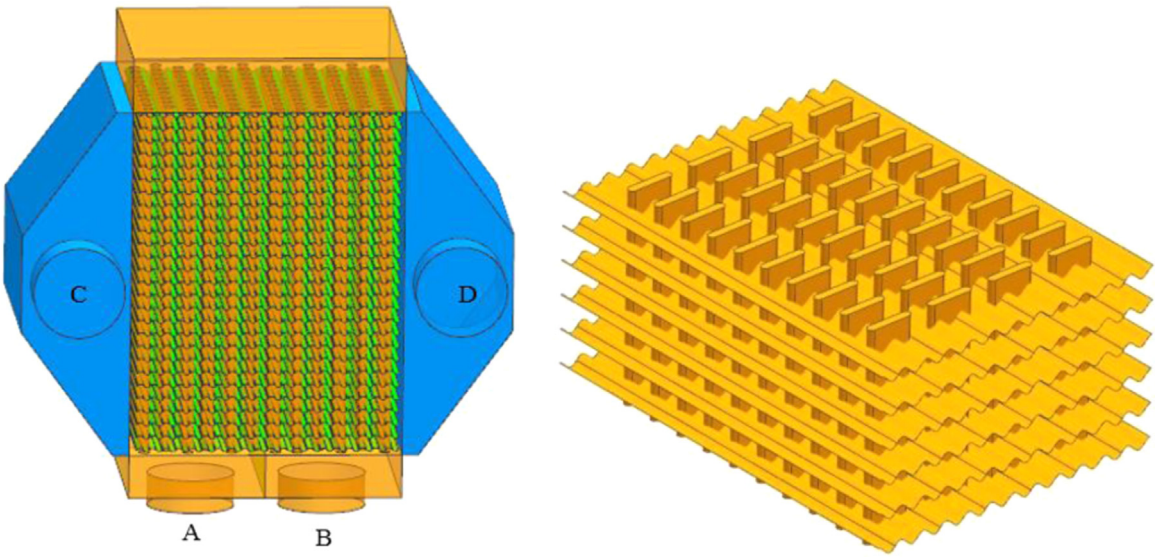

Fig. 1. Geometrical structure of the intercooler.

Table 1
Geometric parameters of intercooler.

Items	Values
Fin thickness (mm)	0.2
Tube wall thickness (mm)	0.6
Water inlet and outlet diameter (mm)	40
Air inlet and outlet diameter (mm)	84
Porous medium region length (mm)	250
Porous medium region wide (mm)	220
Porous medium region high (mm)	320
Material of fin	Aluminum
Material of tube	Copper

the wavy fins, which are substituted with the porous media model in order to decrease the computing quality. The geometry parameters and materials of the actual product used in this study are given in Table 1. Analyzing flow could make calculations to predict flow resistance characteristics using the CFD method. In this study, the heat transfer between fluid domain and solid domain was calculated conjointly.

The periodic unit model of the intercooler consisting of air flow passage and extensions was established shown in Fig. 2 (a). Analyzing flow characteristics could make calculations to predict flow resistance characteristics using the CFD method for the porous model. The whole simulation model including porous medium model is shown in Fig. 2(b).

2.2. Governing equations

The governing equations for continuity, momentum and energy can be expressed as follows:
Continuity equation [13,14]:

$$\frac{\partial}{\partial x_i}(\rho u_i) = 0 \tag{1}$$

Momentum equation:

$$\frac{\partial}{\partial x_i}(\rho u_i u_k) = \frac{\partial}{\partial x_i}\left(\mu \frac{\partial u_k}{\partial x_i}\right) - \frac{\partial p}{\partial x_k} \tag{2}$$

Energy equation:

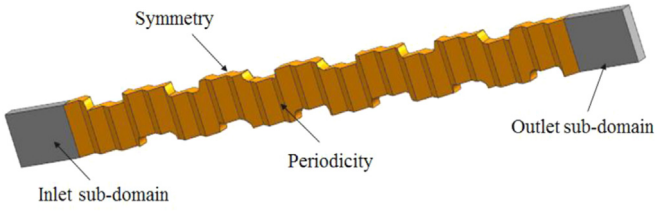

(a) Periodic unit model

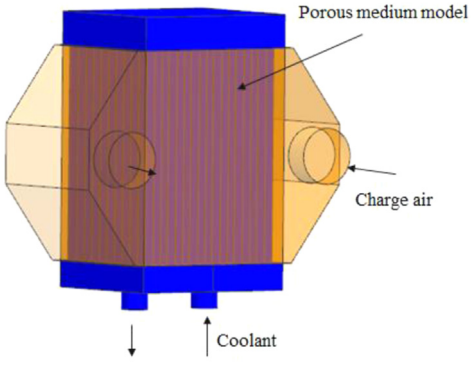

(b) Whole heat exchanger model

Fig. 2. Three-dimensional diagram of the computational domain. (a). Periodic unit model, (b) Whole heat exchanger model.

$$\frac{\partial(\rho u_i u_j)}{\partial x_j} = -\frac{\partial p}{\partial x_i} + \frac{\partial}{\partial x_j}\left(\mu\frac{\partial u_i}{\partial x_j} - \rho u_i u_j\right) \tag{3}$$

Source term equation of porous media model:

$$S_i = -\left(\sum_{j=1}^{3} D_{ij} u v_j + \frac{1}{2}\sum_{j=1}^{3} C_{ij}\rho|v|v_j\right) \tag{4}$$

The pressure drop and the inlet velocity correlations:

$$\Delta p = av^2 + bv \tag{5}$$

Where Δp is the pressure drop from the channel inlet to outlet; v is the inlet velocity.

The effective thermal conductivity in the porous medium is calculated as the volume average of the fluid conductivity and the solid conductivity:

$$k_{eff} = \gamma k_f + (1-\gamma)k_s \tag{6}$$

where γ is the porosity of the medium; k_f is the fluid phase thermal conductivity; k_s is the solid medium thermal conductivity.

The- total heat transfer rate can be calculated as shown below [15]:

$$Q = C_p{\cdot}M{\cdot}(T_{out} - T_{in}) \tag{7}$$

Where Q is the heat transfer rate, the T_{in} and T_{out} are the inlet and outlet temperatures, respectively. M is the mass flow rate.

2.3. Boundary conditions

The boundary conditions for solving above governing equations are specified as follows:

- Inlet boundary condition: The charge air enters from left surface between two fins. The charge air is assumed to have the uniform mass flow rate and constant temperature. The air inlet temperature at the inlet is 20 °C. The range of *Re* is from 1000 to 5000.
- Outlet boundary condition: The outlet is set as a pressure boundary condition, which means that pressure and backflow are specified.
- Symmetry boundary condition: Front-back surfaces of the computational domain model are treated as symmetric and top-bottom surfaces are treated as periotic.
- Wall boundary condition: The solid surfaces are set as nonslip and coupled. The constant temperature (T=21 °C) of inner wall of the tubes is assumed. The material of fins and tubes is aluminum, which has a density ρ=2700 kg/m^3, thermal conductivity k=220 W/(m·k), and specific heat C_p=870j/(kg·k). The working fluids are water and charge air that their thermal properties depend on the temperature.

The air is assumed to have the uniform mass flow rate and constant temperature. The velocity range at the inlet is from 6 m/s to 20 m/s. The outlet is set as a pressure boundary condition, which means that pressure and backflow are specified. Front-back surfaces of the unit computational domain model are treated as symmetric and top-bottom surfaces are treated as periotic. The flow pressure drop and entrance velocity correlation were obtained through the unit simulation shown in

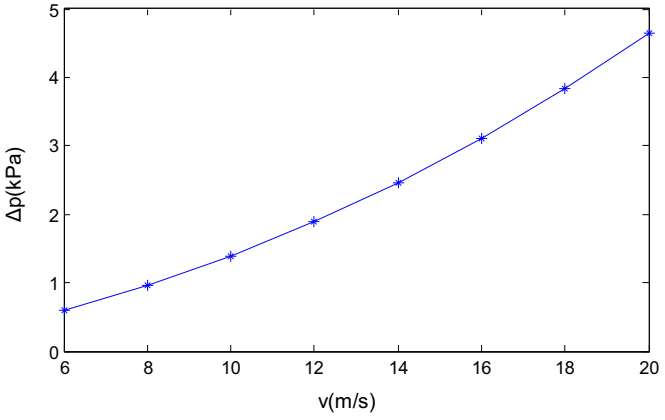

Fig. 3. Simulation result of periodic model.

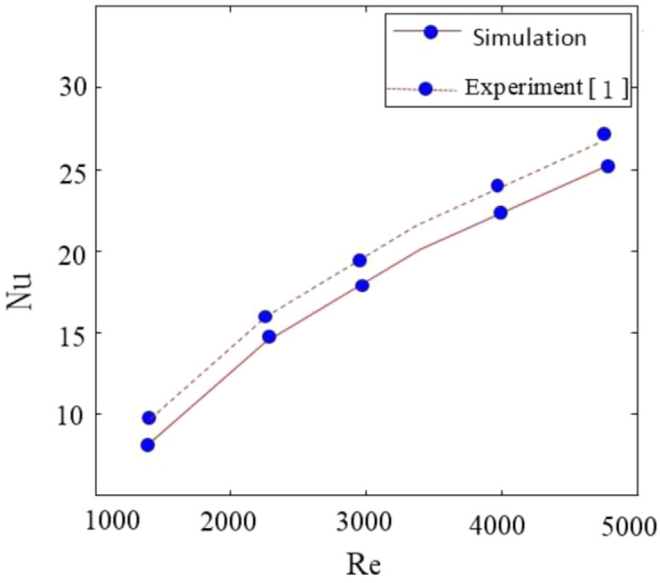

Fig. 4. Variation of Nu with Re.

Fig. 3. According to the formula (5), the values of the viscous resistance coefficient and inertial resistance coefficient are obtained which was provided for the use of the porous medium model. Finally, the viscosity coefficient and inertia coefficient values are determined as 8.5e-6 and 40, respectively. Meanwhile,the porosity of the porous region is defined as 0.9.

3. Results and discussion

3.1. *Effect of Re on Nu*

The different boundary conditions have further effects on pressure drop and heat transfer performance [16]. The computation is conducted for the two-row case with the fin pitch and the corrugation angle being 1.5 mm and 10°, respectively. Fig. 4 shows the characteristics of Nusselt number and friction factor with respect to the Reynolds number. In Fig. 4, the horizontal axis is the *Re*, the left vertical axis is the *Nu*. As can be seen that the Reynolds number ranges from about 1300–4800, corresponding to the inlet velocity from 5 m/s to 20 m/s. Fig. 4 shows the Nusselt number increases almost linearly when the Reynolds number is raised. The maximum simulation and test values of the *Nu* number are 24.5 and 26.2, respectively. Meanwhile, the comparisons of the simulation results and experimental results are provided. It can be seen that the simulation results of the *Nu* are in good agreement with the test results of Dong [1], with the maximum deviation being less than 10%. Comparison results show that the calculation model is accurate and the research method is feasible.

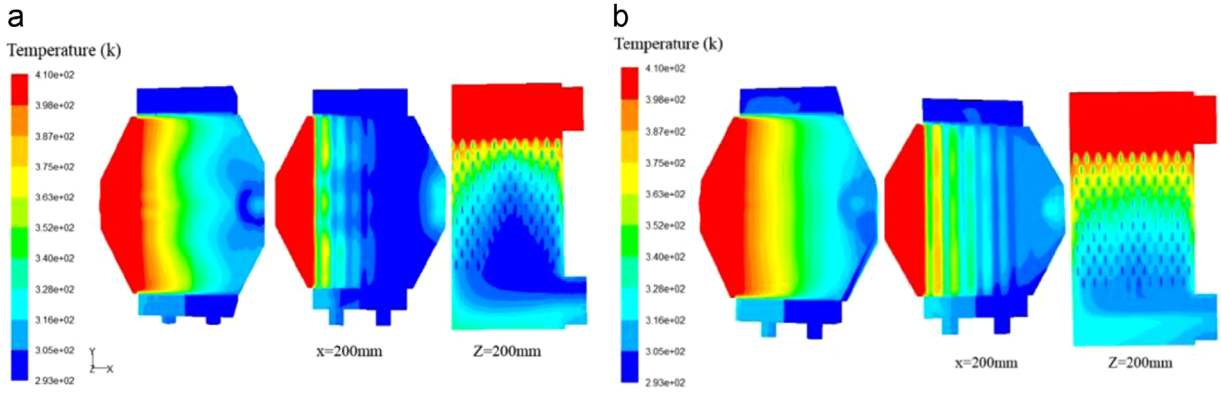

Fig. 5. Temperature contour distribution (a) air mass flow rate 800 kg/h, (b) air mass flow rate 1050 kg/h.

3.2. Flow field and thermal field

In the present investigation, the numerical simulation was carried out to study the flow and heat transfer performance of the intercooler under the different mass flow rates and temperatures. The working fluids in the intercooler are charged air and water, respectively. The cold water inlet (B) boundary conditions were set as 20 °C and 4.2 m³/h. The heat transfer between fluid domain and solid domain was calculated conjointly. Take one case (Q_{air}=1050 kg/h ; T_{air}=137 °C) for example, the distribution characteristics of the pressure and temperature inside the intercooler are obtained as follows.

Fig. 5 shows the temperature distribution of the hot air and cold water inside the intercooler. The high temperature air is cooled by cold water in the pipes through the tube walls. As expected, high inlet temperature as well as high gradients appear in the flow direction, especially in the inlet regions. Therefore, the high temperature region is subjected to big thermal stresses. Reducing thermal stresses would be an important aim for optimal structural design. The air temperature along the flow direction reduce gradually, however, the water temperature is becoming higher and higher along the tubes from the cross section (x=200 mm). It could also be observed from the cross section (z=200 mm) that the fins are heated and only a very thin layer of air is cooled after first entering the channel. The largest temperature changes in this model occur in the low-velocity zones just after each of the tubes. Furthermore, it is also found that the high temperature regions occur in the middle of the two tubes, meanwhile, the low temperature regions occur near the fins and tubes due to the high heat transfer coefficient which enhance the heat transfer. Thermal stratification of the solid materials is significant and the outlet temperature value is the lowest. In Fig. 5(b), the minimum temperature value of the exit at the air side is 44 °C, and the air temperature decreases about 90 °C. The total temperature differences of the water from the inlet to the outlet is about 10 °C. The authors found that reducing the air mass flow rate would lead to a reduction in the temperature gradients, but they still occur in the inlet region. It is clear to see that the air temperature value of the entrance is lower with increasing air mass flow rate by comparison. This is because of the higher heat exchange efficiency between the tube walls and the charge air as a result of lower air density and velocity.

Fig. 6 shows that the pressure has a gradient descent trend in the air side along the flow direction, which is very similar to the temperature change trend. Also, the highest pressure occurs at the last part of the entrance where is close to the water pipes from the cross section (z=200 mm). This is because the air velocity is very fast and has great inertia. It can be clearly seen by comparison that the bigger the inlet mass flow rate, the higher the pressure at the entrance. The pressure load could cause stress which can damage the connection of the fins and tubes. Therefore, it should pay more attention in the design which could affect the solder quality in developing new products. The air flows along the y direction with the pressure drop along the flow passage by almost 600 Pa and 800 Pa, respectively. As shown from the cross section (x=200 mm), the maximum pressure in the cold fluid side occurs at the entrance with the pressure drop along the flow channel by almost 3.2 kPa.

3.3. Flow uniformity analysis

As we all know, the more uniform the mass flow rate distribution through all pipes, the higher the heat transfer capacity of the whole intercooler. They found that flow maldistribution in the headers affected the exchanger performance. Hence, it is very important to the analysis of the inlet flow uniform. Fig. 7 depicts the distribution of the mass flow rate in all those tubes. There are altogether 63 flat pipes at the entrance of the cold fluid side. It can be seen that the mass flow rates are distributed almost symmetrically. The range of the mass flow rate in each tube is from 0.16 kg/s to 0.23 kg/s, respectively. The flow rate in the middle of the header is larger than others. Furthermore, the maximum flow rate of all the tubes appears at the bottom of the header. The maximum deviation of the mass flow rate between the average value and the simulation values is less than 10% and more than 85% have errors lower than 8%, which demonstrates that the flow distribution through the pipes is almost uniform.

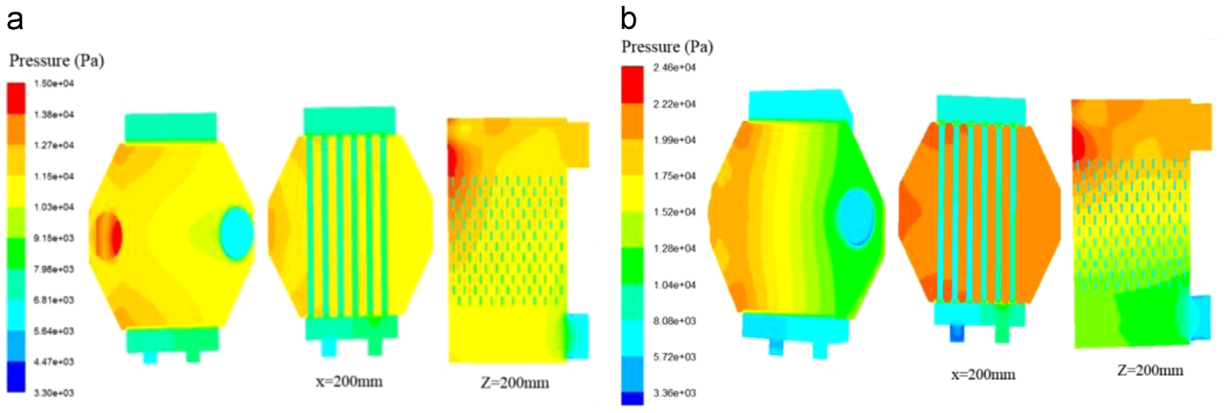

Fig. 6. Pressure contour distribution (a) air mass flow rate 800 kg/h, (b) air mass flow rate 1050 kg/h.

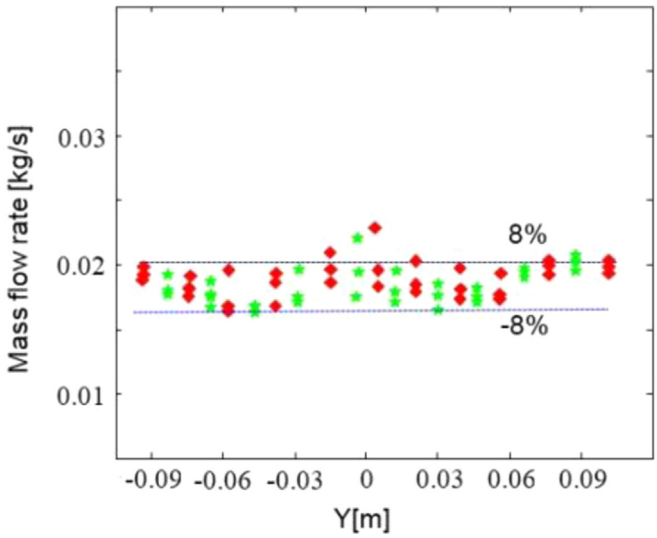

Fig. 7. Water mass flow rate distribution in each tube.

3.4. Effect of coolant on heat transfer performance

In order to study the effect of the water flow ways to heat-exchange characteristic, the paper made an analysis of the heat transfer rate of the overall heat transfer model. The air flow direction is from C to D. Also, the water flow inlets are A and B, respectively. In Fig. 8, the horizontal axis is the water mass flow rate, the left vertical axis is the heat transfer rate. It is very obvious that the overall heat transfer rate is increased in exponent regularity with the increase of the water mass flow rate. The heat transfer rate, which the inlet is B could increase by almost 10% than that the inlet is A. Results indicate that the coolant flow directions have a significant impact on the heat exchange performance of the intercooler.

4. Experimental verification

The test apparatus used in this study is shown in Fig. 9. It mainly consists of the supercharged diesel engine, the intercooler, water circulation and control unit and data acquisition system situated in a constant temperature laboratory. Air and water are used as the working fluid. The mass flow rate and temperature are regulated by the water circulation and the control unit. The water loop is composed of a water tank, an electric heater (150 kW), a water pump and a temperature controller. Water temperatures at the entry and exit are measured by the platinum resistance temperature sensors (Pt-100)

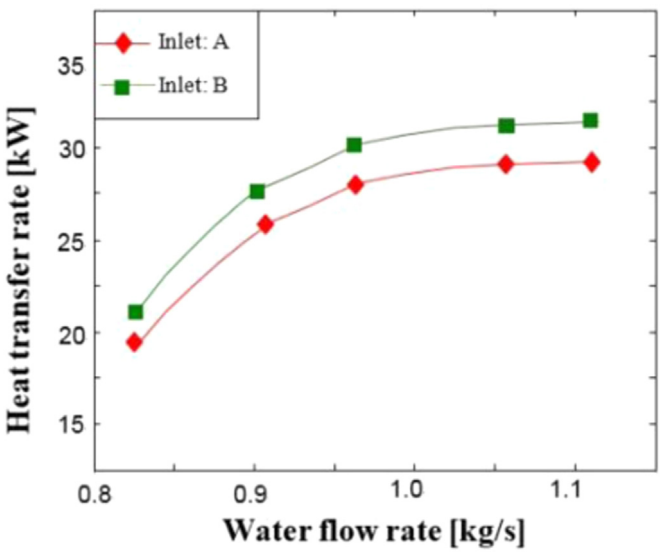

Fig. 8. Effect of water flow directions on the heat transfer rate.

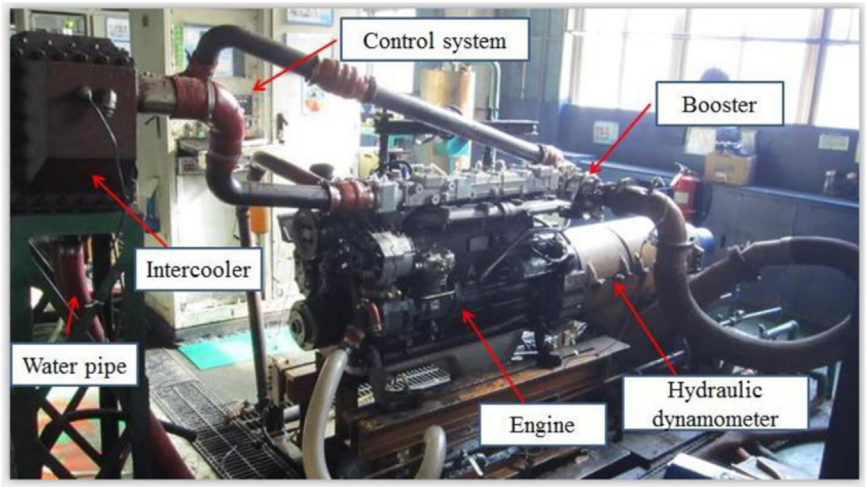

Fig. 9. Test apparatus to study the intercooler.

which accuracy is within 0.1%. In addition, the air temperature is measured by CYZ103 high temperature pressure sensors which accuracy is within 0.4%. The main influencing factors studied in this article on heat transfer performance include coolant flow rate and coolant temperature. The heat transfer performance can be varied by regulating the coolant flow rate and temperature in the experiment. Coolant temperature are constant keeping at 30 °C in the bench test. The air temperature and used to calculate the heat transfer rate were measured listed in Table 2.

According to the formula (7), the values of heat exhage rate are calculated, and the comparisons of the simulation values and experimental data are provided in Fig. 10. Results in Fig. 10 (a) show that the maximum deviation is less than 15% with the average deviation of 6.5% of all measured values by comparison. It is clearly seen that the heat transfer power are increased with the increase of charge air mass flow.However, the increase rate for simulation values is greater than the experimental values. Comparison results show that the calculation model is accurate and the research method is feasible. Thus, the model can be utilized for further analysis and the results could be used as a reference for further optimal design.

5. Conclusion

In the present study, the calculation model based on the porous media theory is developed to predict the flow field and temperature field of the intercooler which is used in the heavy-duty diesel engine. Detailed study of the heat transfer performance has been conducted under the different boundary conditions. Conclusions are summarized as follows:

(1) Get the flow field and temperature field inside the intercooler under the different air mass flow rates. Results show that the air mass flow rate has an important influence on the heat exchange efficiency. The part which has the largest thermal stress is found by simulation, and the stress is bigger with the increase of air flow rate. The simulation results show that the porous medium model could effectively investigate the fluid flow and heat exchange in the intercooler.
(2) Obtain the change trend about the effects of mass flow rates on the total heat exchange performance under the different conditions. The difference of the heat transfer rate under the two heat exchange types is almost 10%. Moreover, the changes of coolant flow rate have a slight influence on the heat transfer rate while the coolant temperature has a significant impact. The simulation results show that the influence of coolant parameters on the overall heat transfer

Table 2
Intercooler bench test results.

v (r/min)	Accelerator (%)	m (kg/h)	T_{in} (°C)	T_{out} (°C)	T (N.m)
2300	100	848	172	46	700
2200	100	803	170	45	730
2100	100	771	167.3	44.8	742
2000	100	748	167.1	44.5	795
1900	100	715	166.6	44	807
1800	100	672	162.6	43.5	802
1700	100	627	157	42.2	805
1600	100	576	149	40	798
1500	100	553	148	38.4	792
1400	100	444	137	36.3	769

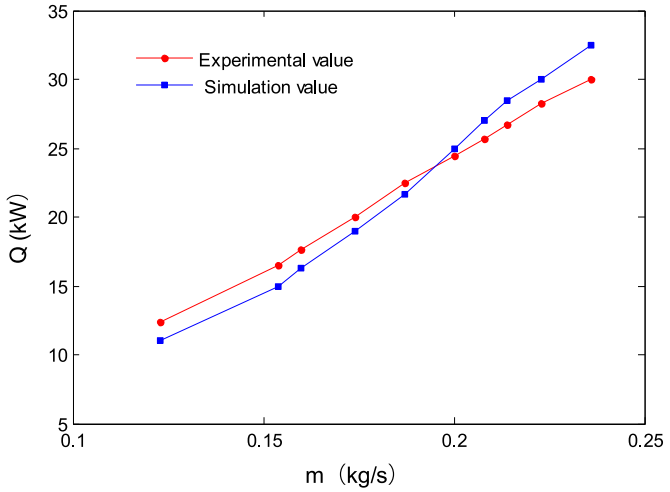

Fig. 10. Comparison of experiment data and predict data.

power not only depends on the inlet temperature but also depend on the mass flow rate. The bigger the coolant flow rate, the more the heat transfer power. And the higher the inlet temperature, the less the heat transfer.

(3) The heat exhage rate are calculated for the wavy fin-and-tube intercooler based on porous model. The simulation results are in good agreement with bench test results within 15%. Experimental data and simulation models used in this paper can be used to estimate the thermal performance of the wavy fin intercooler during the initial design phase.

References

[1] J.Q. Dong, L. Su, Experimental study on thermal-hydraulic performance of a wavy fin-and-flat tube aluminum heat exchanger, Appl. Therm. Eng. 51 (2013) 32–39.
[2] C. Oliet, A. Oliva, Parametric studies on automotive radiators, Appl. Therm. Eng. 27 (2007) 2033–2043.
[3] Shon Jungwook, Kim Hyungik, Improved heat storage rate for an automobile coolant waste heat recovery system using phase-change material in a fin-tube heat exchanger, Appl. Energy 113 (2014) 680–689.
[4] J. Wen, Y.Z. Li, A.M. Zhou, PIV experimental investigation of entrance configuration on flow maldistribution in plate-fin heat exchanger, Cryogenics 46 (2006) 37–48.
[5] A.J. Jiao, R. Zhang, Experimental investigation of header configuration on flow maldistribution in plate-fin heat exchanger, Appl. Therm. Eng. 23 (2003) 1235–1246.
[6] M.A. Habib, R.B. Mansour, S.A.M. Said, Evaluation of flow maldistribution in air-cooled heat exchangers, Comput. Fluids 38 (2009) 677–690.
[7] L.S. Ismail, Numerical study of flow patterns of compact plate-fin heat exchangers and generation of design data for offset and wavy fins, Int. J. Heat. Mass. Transf. 52 (2009) 3972–3983.
[8] Y.L. He, W.Q. Tao, Three-dimensional numerical study of heat transfer characteristics of plain plate fin-and-tube heat exchangers from view point of field synergy principle, Int. J. Heat. Mass. Transf. 26 (2005) 459–473.
[9] Z. Qi, J. Chen, Parametric study on the performance of a heat exchanger with corrugated louver fins, Appl. Therm. Eng. 27 (2007) 539–544.
[10] Q.W. Wang, Q.Y. Chen, G.D. Chen, Numerical investigation on combined multiple shell-pass shell-and-tube heat exchanger with continuous helical baffles, Int. J. Heat. Mass. Transf. 52 (2009) 1214–1222.
[11] Y.P. Chen, Y.J. Sheng, Numerical simulation on flow field in circumferential overlap trisection helical baffle heat exchanger, Appl. Therm. Eng. 50 (2013) 1035–1043.
[12] A.A. Masri, M. Peksen, L. Blum, A 3D Model for predicting the Temperature Distribution in a Full Scale APU SOFC Short Stack under Transient operating conditions, Appl. Energy 135 (2014) 539–547.
[13] J.M. Wu, W.Q. Tao, Effect of longitudinal vortex generator on heat transfer in rectangular channels, Appl. Therm. Eng. 37 (2012) 67–72.
[14] (FLUENT, v6).3 User Manual. Fluent Inc. New Lebanon, NH, 2008.
[15] A.M. Hussein, R.A. Bakar, Heat transfer enhancement using nanofluids in an automotive cooling system, Int. J. Heat Mass Transf. 52 (2014) 1–8.
[16] Y. Sui, C.J. Teo, Fluid flow and heat transfer in wavy microchannels, Int. J. Heat Mass Transf. 53 (2010) 2760–2772.